Available online at www.HEFJournal.org

ISSN: 2785-2997

Journal of
Human, Earth, and Future

Vol. 6, No. 2, June, 2025

Optimizing Concrete Mix Design for Cost and Carbon Reduction Using Machine Learning

Angga T. Yudhistira [1], Arief S. B. Nugroho [1*], Iman Satyarno [1], Tantri N. Handayani [1], Malindu Sandanayake [2], Rimba Erlangga [3, 4], Jonathan Lianto [5], Alfa Rosyid Ernanto [1]

[1] *Department of Civil and Envinromental Engineering, Universitas Gadjah Mada, Sleman, Indonesia.*

[2] *Institute of Sustainable Industries and Liveable Cities, Victoria University, Melbourne, VIC 3011, Australia.*

[3] *Department of Computer Science and Electronics, Universitas Gadjah Mada, Sleman, Indonesia.*

[4] *PT Fliptech Lentera Inspirasi Pertiwi, Indonesia.*

[5] *PT Adhi Karya Persero Tbk, Indonesia.*

Received 21 December 2024; Revised 11 May 2025; Accepted 16 May 2025; Published 01 June 2025

Abstract

Cement is the main component of concrete and one of the most significant contributors to carbon emissions. Reducing cement use can significantly reduce global carbon emissions. This study aims to create an optimal concrete mixture of cost and minimal carbon emissions, but the compressive strength meets the requirements. XGBoost Machine Learning Algorithm is used to make predictions, and PSO is used to obtain the optimal mixture. The novelty of this study is the presence of concrete age variables, determination of PSO parameter weights using stakeholder preference analysis of construction in Indonesia with the AHP method, and validation of the PSO-recommended mixture using laboratory tests, which is still rarely done. The research findings indicate that the ML model provides satisfactory prediction values with an R^2 value of 0.9043, root mean square error of 48.5147 and mean absolute percentage error of 0.0484. PSO results show that cement reduction in concrete can be achieved with optimal use of admixture while reducing 1-3% costs and 7-10% carbon emissions. The research findings provide critical insights into the importance of using innovative techniques to optimize sustainable concrete mixes, accelerating the market implementation of products with cost benefits.

Keywords: Concrete; Machine Learning; Strength Prediction; Carbon Reduction; Cost Reduction.

1. Introduction

The consequences of global warming have been witnessed in numerous regions of the country in Southeast Asia, such as extreme heat, high air pollution, etc. Many efforts have been undertaken to reduce carbon emissions to mitigate global warming, and construction is no exception. Globally, 30% to 40% of greenhouse gas (GHG) emissions were caused by construction projects [1]. Concrete is the primary construction material used in the construction industry, and over 50% of structural materials used worldwide are still made of concrete [2]. Roughly 5% to 7% of the carbon emissions originate from cement manufacture, predominantly used in concrete materials [3]. Cement, the main component of concrete, contributes the most to carbon emissions per ton, with an approximate value of 0.9 tons of CO_2/ton of concrete). Therefore, it is essential to investigate the possibilities of reducing cement in concrete while maintaining compressive strength [4, 5].

* Corresponding author: arief_sbn@ugm.ac.id

http://dx.doi.org/10.28991/HEF-2025-06-02-04

Previous studies have extensively focused on replacing 100% cement in concrete and introducing novel concretes like geopolymer concrete, an alternative to ordinary Portland Cement Concrete (OPC) [6]. However, issues on the workability and economic value of geopolymer concrete still exist, limiting its broad usage within the construction industry; often, the price of these geopolymers can be up to twice as high [7]. Despite a projected 44.64% GHG reduction compared to OPC concrete, an optimization-based study conducted in Melbourne utilizing fly ash geopolymer concrete showed reductions of GHG emissions and production costs could be in the range of 3.63%–41.57% and 23.80%–30.25% respectively [8].

A different approach to reduce the requirement for cement and optimize the mix design is to create a low-carbon composition by optimizing various additional components such as concrete admixture [9]. Optimization refers to minimizing or maximizing a function within a specified set of feasible alternatives in a specific context. The tool facilitates the comparison of different alternatives to select the most suitable option. Artificial intelligence (AI) technology is among the many methods available for optimization. However, optimization using manual computations is challenging when more extensive data sets are associated. AI is a popular option for performing complex modeling tasks that include large amounts of data that are challenging to accomplish through manual computations. AI enables the rapid generation of multiple iterations with high computational precision. Machine learning (ML) algorithms can accurately forecast the compressive strength of cement-based materials with high accuracy and learning capacity [10, 11]. A study revealed that applying machine learning in mix design optimization could lead to a 10% decrease in cement consumption, resulting in a corresponding 10% reduction in carbon emissions [12]. Another study utilized the combination of gradient boosting (GB) and particle swarm optimization (PSO) to execute multi-objective optimization on geopolymer concrete mix designs, which resulted in a production cost efficiency improvement that varied from 7.6% to 27%, as well as a significant reduction in carbon emission values from 77.3% to 81.3% [13]. It has also been proven that many variations of concrete mixture composition can produce the same compressive strength, resulting in different embodied carbon values, even for high compressive strength [9]. Another study in Korea utilized an evolutionary algorithm (EA) to evaluate the effectiveness of a low-carbon concrete mix design system, revealing that the optimal design reduced CO_2 emissions by 4% and 7%, respectively [14]. Nevertheless, specific structural components' optimal cost and eco-efficiency combinations may significantly differ [15].

Another similar study utilized machine learning called gene expression programming (GEP) to forecast the compressive strength of concrete. The study employed rice husk ash, ceramic waste powder, and glass waste powder as alternative cement replacements with R-values of 0.95, 0.93, and 0.89 for training, testing, and validation, respectively, demonstrating high accuracy and reliability in implementation [16]. Another study employed an artificial neural network (ANN) to forecast self-compacting concrete (SCC) properties containing silica fume and fly ash at varying stages of maturity, resulting in a correlation coefficient of 0.9835 [17]. Similarly, various ML algorithms, which included ANN, extreme gradient boosting (XGBoost), support vector regression (SVR), and adaptive neuro-fuzzy inference system (ANFIS), were employed to predict the performance of recycled aggregate. These previous studies indicate that XGBoost is the better optimal algorithm for predicting compressive strength, with a deviation of less than ±10% [18–25]. XGBoost achieves optimal performance by improving regularization to prevent overfitting due to model complexity [26].

Thus, the current research uses The XGBoost machine learning (ML) algorithm to predict the compressive strength at a particular age combined with particle swarm optimization (PSO) framework to acquire a specific concrete composition that fulfills the desired objective. Historical data from laboratory testing results are modeled using the XGBoost algorithm to predict compressive strength values at a certain age. XGBoost is used because previous studies have shown that this algorithm is superior in predicting concrete compressive strength compared to other ML algorithms. Optimization is conducted by considering compressive strength, production costs, and carbon emissions using PSO. The simulation results are later validated with laboratory testing. Although many previous studies have used ML to predict concrete compressive strength, the novelty of this study is the addition of concrete age variables that are still rarely studied. In addition, in previous studies using PSO, the weight of each category was determined by the researcher himself. Still, in this study, the weight is obtained from the results of a preference study using the Analytic Hierarchy Process (AHP) method on construction stakeholders in Indonesia. In this study, validation of the PSO-recommended mixture using laboratory tests was also done. The research can guide construction stakeholders in formulating a plan identifying the most advantageous concrete mixture, ensuring superior quality while minimizing costs and carbon emissions. This approach is particularly important for rapidly industrializing countries like Indonesia to promote sustainable practices as it prepares for large-scale growth of the construction industry in the coming years.

2. Background

Numerous predictive modeling studies have been conducted to determine the compressive strength of concrete using various additives and algorithms. A literature review containing 60 Scopus-indexed Q1 journals published between 2020 and 2024 was conducted. The focus of the selected papers included the prediction and optimization of concrete mixture composition using ML approaches. Figure 1 illustrates the distribution of ML research on predicting and optimizing concrete compressive strength. The results of these investigations revealed the utilization of over 31 algorithms and 18 different types of materials, as detailed in Table 1.

The literature review revealed that the studies related to predicting the compressive strength of concrete are primarily carried out on standard concrete and alkali-activated materials (geopolymer). Along with developments in construction material technology, studies on the prediction and optimization of compressive strength with various alternative materials, such as RCA, SCC, bio-composite aggregate, nano silica, magnesium silicate, magnesium phosphate, and plastic aggregate, have begun in multiple regions. However, the opportunity to explore these topics is still vast, considering that the concrete component materials in each area have different characteristics. The use of Random Forest (RF), Neural Network (NN), XGBoost, Decision Tree/Regression Tree (DT/RT), GB, Support Vector Machine (SVM), SVR, and Linear Regression (LR) ML algorithms were found to be the most frequently used in recent research. Nevertheless, additional machine learning techniques are now being investigated and hold promise for addressing decision-making challenges. Several machine learning algorithms included in this list are Light Gradient-Boosting Machine (Light GBM), K-Nearest Neighbor (KNN), Gaussian Process Regression (GPR), Ada Boost (AB), GEP, and Ridge Regression (RR). In the future, the study of these algorithms still has excellent potential. Given that Machine Learning can rapidly create large amounts of data through simulations, it dramatically facilitates decision-making for people.

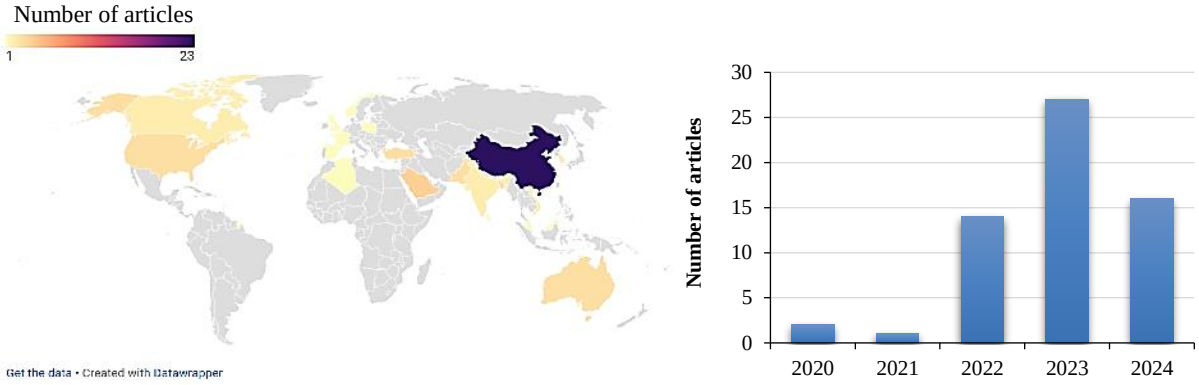

Figure 1. Country distribution of studies on predicting and optimizing concrete compressive strength using ML

Despite several studies undertaken, the research on addressing strategies to mitigate the effects of global warming, particularly in Indonesia, is still limited. This analysis is crucial because it can support the goals of various countries in achieving decarbonization targets by 2030, contributing to the achievement of the SDGs. Most studies apply some historical data, which were not used as training data but predominantly as validation data. Considering that the concrete constituents vary significantly in each region, the compressive strength results of concrete in one region are unique and different from those in other regions, even with the same composition. Many studies have conducted laboratory validation tests on new design mixes using ML predictions. However, there are still few studies that have focused on both optimization and validation. In the present research, laboratory validation tests were also carried out to determine actual compressive strength value errors from test results and predictions using PSO datasets generated from the optimization process. This approach is vital to justify the reliability of the ML prediction model for application in the field.

Table 1. Research distribution considering the type of material used

Type of Material	ML Algorithm	Frequency	Source
Normal Concrete	RF	11	[12, 26, 27–34, 35]
	NN	10	[4, 12, 27, 30, 32, 36–40]
	XGBoost	12	[24, 25, 26, 28–31, 33–35, 40]
	GB	8	[24, 26, 28–32, 40]
	DT/RT	7	[12, 24, 25, 30, 32, 35, 37]
	SVM	4	[4, 27, 30, 41]
	SVR	6	[31–33, 36, 37, 42]
	LR	3	[32, 37, 41]
Alkali-Activated Material (Geopolymer)	RF	8	[13, 19, 43–48]
	NN	7	[13, 43, 44, 46–49]
	XGBoost	3	[19, 45, 48]
	DT/RT	2	[47, 50]
	GB	4	[13, 45–47]
	SVM	4	[43, 44, 46, 47]

Recycle concrete aggregate (RCA)	RF, DT/RT	3	[51–53]
	NN	4	[22, 51–53]
	XGBoost, GB	3	[51, 52, 54]
	SVR	2	[51, 54]
	LR	1	[51]
Self-Compacting Concrete (SCC)	RF	3	[55–57]
	NN, SVM	2	[55, 56]
	XGBoost	3	[20, 55, 57]
	DT/RT	4	[20, 55–57]
	GB	2	[20, 55]
High strength concrete (HSC)	RF	1	[58]
	NN, SVM, DT/RT, LR	2	[9, 58, 59]
	XG Boost	1	[59, 60]
Calcined sludge/clay cement	RF,NN, SVM, SVR, DT/RT, LR	1	[61]
	XGBoost	1	[62]
Steel Fiber Reinforced Concrete (SFRC)	RF, SVR, DT/RT, GB	1	[63]
	NN	1	[64]
lightweight concrete	RF, SVR, LR	1	[65]
Mortars	SVM	1	[66]
Reactive Powder Concrete	RF, DT/RT, XGBoost	1	[67]
Nano silica concrete	RF, NN, SVM, DT/RT, LR	1	[68]
Magnesium silicate hydrate cement	RF, SVR, DT/RT, LR, GB	1	[69]
Cement-based material	RF, SVR, LR, XGBoost	1	[21]
Bio-composite aggregate concrete	NN	1	[70]
Strain-hardening cementitious composites (SHCC)	SVM, XGBoost	1	[71]
Coral Aggregate Concrete	NN	1	[72]
Plastic Aggregate Concrete	RF	1	[73]
Magnesium phosphate cement	NN, SVR, DT/RT, LR, GB, XGBoost	1	[74]

RF: Random Forest, NN: Neural Network, SVM: Support Vector Machine, SVR: Support Vector Regression, DT/RT: Decision Tree/Regression Tree, LR: Linear Regression, GB: Gradient Boost, XGBoost: Extreme Gradient Boost.

3. Data and Method

A total of 132 datasets were acquired from historical testing data in the laboratory. Table 2 illustrates the range of the test data utilized. Scheme 0 is a control variable, where the compressive strength target is 30 MPa, and a water content ratio (wc ratio) of 0.5 was used without adding admixture. Scheme 1 uses the same composition as scheme 0 but adds admixture at doses of 0.2% and 2.0%, indicating minimum, average, and maximum doses. In scheme 2, water content is reduced to alter the wc ratio. Meanwhile, in scheme 3, the use of water and cement is reduced to maintain the same wc ratio, but the use of cement is reduced.

Sulfonated naphthalene formaldehyde (SNF)-based admixture has been used in this research, considering its three functions: 1) increased workability, without change composition; 2) reduced wc ratio to increase strength and improve durability; 3) reduced water and cement at given workability to prevent creep, shrinkage, and thermal strain due to cement hydration [75]. The cement utilized is of the Ordinary Portland Cement (OPC) variety, with the fine aggregates having a unit weight of 1400 kg/m^3 and a silt content of 4.40%. The coarse aggregates have a unit weight of 1385 kg/m^3 and a Los Angeles abrasion test result of 16.80%.

Table 2. Experimental Specimen Range (for 1 m^3 concrete)

Parameter	Units	Test scheme									
		0	1A	1B	1C	2A	2B	2C	3A	3B	3C
fc'	Mpa	30	30	30	30	30.47	37.81	40.84	30	30	30
Water content	L	205	205	205	205	203	174	164	203	174	164
wc ratio	-	0.50	0.50	0.50	0.50	0.50	0.43	0.40	0.50	0.50	0.50
Cement	kg	408	408	408	408	408	408	408	404	347	327
Fine aggregates	kg	715	715	715	715	716	727	731	717	752	764
Coarse aggregates	kg	1072	1072	1072	1072	1073	1091	1097	1076	1127	1146
Admixture content	%	0.00%	0.20%	1.10%	2.00%	0.20%	1.10%	2.00%	0.20%	1.10%	2.00%

Compressive strength and slump data obtained through laboratory tests are shown in Table 3. Compressive strength tests were conducted at 1 day, 3 days, 7 days, and 28 days. This technique intends to estimate the concrete compressive strength at an early age or a certain age. The data obtained from testing are applied to create a compressive strength prediction model using the XGBoost algorithm. The modeling results are displayed in a frontend application, which facilitates predictions using large datasets or individual data inputs. This prediction model is then used to optimize and obtain a design mix composition that fulfils the strength requirements; it is the most cost-effective and has the lowest carbon emissions.

A study in Indonesia found that construction stakeholders prioritize quality (63.33%), cost (26.05%), and carbon emissions (10.62%), with data from 35 respondents across Indonesia gathered using the AHP [76]. The weights factor obtained from the research is used as the basis for weights in PSO modeling. Slump loss tests were also conducted to observe the slump loss characteristics of each composition. The PSO algorithm obtains the most optimal mixture composition according to the desired criteria. The results of this optimization were revalidated using laboratory tests with the design mix as the PSO output to identify the deviation between the AI modeling outcomes and the field results. The complete research process is presented in Figure 2.

Table 3. Compressive test and slump result from laboratory experiment

Skema	Water (L)	Cement (kg)	Fine aggregate (kg)	Coarse aggregate (kg)	Admixture (kg)	fc' (Mpa)				
	X1	X2	X3	X4	X5	Y1	Y2	Y3	Y4	Y5
						1 day	3 days	7 days	28 days	Slump
0	204.85	408	704	1056	0	12.49	23.31	27.52	33.15	8
1A	204.85	408	704	1056	0.82	11.97	18.29	28.37	34.51	11
1B	204.85	408	704	1056	4.49	12.46	20.82	26.46	37.46	23
1C	204.85	408	704	1056	8.16	12.65	22.22	23.17	36.99	22
2A	202.79	407.95	705	1058	0.82	17.45	28.06	31.14	43.16	9.5
2B	174	408	716	1075	4.49	22.79	34.48	39.99	52.01	4.5
2B-1	192	408	716	1075	4.49	17.9	28.53	33.88	42.17	10
2C	164	408	721	1081	8.16	25.38	34.67	50.06	52.18	10
3A	203	404	707	1060	0.82	11.97	26.05	36.93	38.6	9.5
3B	174	347	741	1111	4.49	14.46	22.94	24.74	34.94	11
3C	164	326	753	1130	8.16	12.3	21.87	25.64	27.2	10

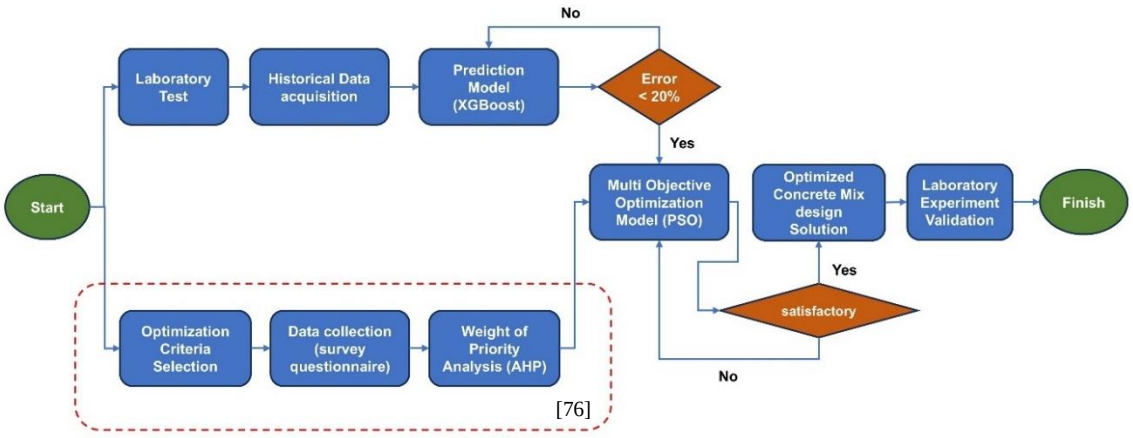

Figure 2. Research process

4. Machine Learning Algorithm

4.1. XGBoost

A limitation of GBoost is its prolonged iteration process and frequent occurrence of overfitting [60]. The XGBoost method was developed to improve the limitations of the GBoost algorithm and mitigate overfitting [77]. As a more advanced iteration of GBoost, the XGBoost algorithm is frequently used for model-classifying regression [78]. This algorithm consists of several decision trees, which are trained using the prediction outcomes of the previous trees. The final result of the model prediction is the summation of the prediction outcomes for each tree, as shown in Equation 1 [78]. The GB and XGBoost algorithms are illustrated in Figure 3.

$$f_i^p = \sum_{k=1}^{l} f_k(x_i) = f_i^{(p-1)} + f_i(x_i) \quad (1)$$

where $f_p(x_i)$ is learner stage p, f_i^p and $f_i^{(p-1)}$ indicates forecast stages p and $p-1$, and x_i denotes the parameter input [60].

4.2. Particle Swarm Optimization

Particle Swarm Optimization (PSO) is an optimization method inspired by the collective behavior of birds flocking or fish schooling. Kennedy & Eberhart first described it in (1995) [79]. The algorithm involves particles moving through a solution space, repositioning themselves according to their optimal position and the best-known positions of their neighbors. Consequently, it can effectively solve complex optimization problems [79]. Variations, such as inertia weight PSO and constriction factor PSO, have been developed to enhance performance by balancing exploration and exploitation [80, 81].

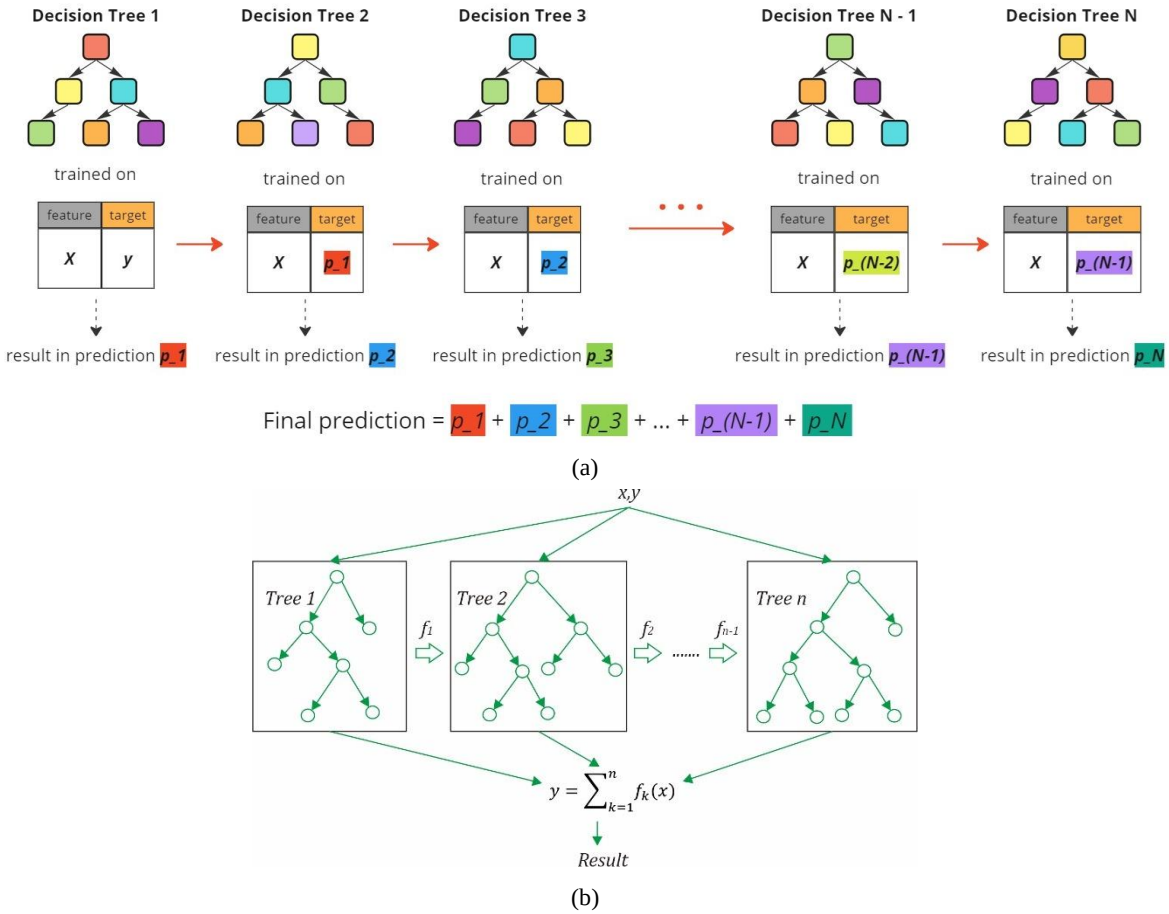

Figure 3. (a) Schematic of GB (b) General architecture of XGBoost [82]

PSO algorithm has demonstrated successful applications in diverse domains, encompassing the areas of engineering, machine learning, and robotics due to its simplicity and efficiency [83]. Comparative studies have shown that PSO often outperforms traditional optimization methods and other metaheuristics, such as genetic algorithms, particularly in terms of convergence rate and quality of solution [84]. However, it can struggle with premature convergence, which has led to the development of hybrid and adaptive versions to improve performance and adaptability [84]. As research continues, PSO is expected to evolve, addressing new challenges and expanding its application scope [83]. The PSO algorithm is illustrated in Figure 4 [13].

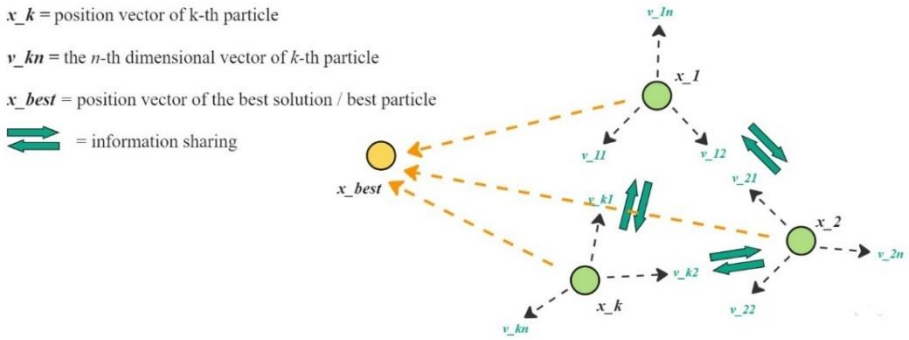

Figure 4. Illustration of the PSO algorithm

5. Compressive Strength Prediction and Optimization Model

The final model is an ensemble of an XGBoost model and a linear regression (LR) model with some weighted averaging, then multiplied by a multiplication factor. One hundred ten (110) data samples were used for training and 22 for validation. The LR model is incorporated to cover the drawbacks of using XGBoost or, generally, a tree-based model, which constantly predicts the target value given some gaps between two feature values. In our case, the feature is the age of the mixture in days. The training data only consists of three, seven, and 28 days. Thus, a tree-based model will result in the exact prediction for a seven-day admixture when new data with an age of 10 days are available. During the training and inference phase, the data is standardized for the linear regression and kept as is for the XGBoost model.

The optimum weight and multiplier are determined using a hyperparameter tuning process in parallel to identify the best model hyperparameter, applying Bayesian optimization within the Optuna library [85]. The tuning objective, as well as the inherent XGBoost objective function, minimize the symmetric mean absolute percentage error (SMAPE) metrics as follows:

$$SMAPE(y,p) = \sum_{i=1}^{N} \frac{|p_i - y_i|}{|p_i + y_i|}, \quad (2)$$

where y_i and p_i represent the i-th actual maximum load and predicted maximum load, respectively.

The tuning results are 0.9 for the XGBoost weight, 0.1 for the LR weight, and 1.08 for the multiplier. The final predicted maximum load of a feature vector x is obtained as follows:

$$f(x) = 1.08 \times (0.9 \times f_{xgb}(x) + 0.1 \times f_{lr}(x)), \quad (3)$$

where $x = (age\_days, diameter, height, wc\_ratio, cement, admixture\_kg, fine\_aggregate\_kg, coarse\_aggregate\_kg)$.

The final equation for the LR model is expressed as follows:

$$f_{lr}(a,d,h,\ldots) = 95.92 \times a - 7.81 \times d - 23.20 \times h - 66.46 \times wcr + 23.37 \times m_C + 7.74 \times m_{ad} + 0.22 \times m_{fa} + 1.51 \times m_{ca} \quad (4)$$

where $a, d, h, wcr, m_C, m_{ad}, m_{fa}, m_{ca}$ denote curing age, cylinder sample diameter, sample height, water–cement ratio, the weight of cement, the weight of admixture, the weight of fine aggregates, and the weight of coarse aggregate, respectively.

The hyperparameter tuning of the XGBoost model results in a learning rate of 0.0747, a maximum depth of 2, and 72 estimators. Although the standalone XGBoost model has better metrics than the final ensemble model, it cannot monotonically increase the prediction results as the age of the mixture rises. The final ensemble model addresses this disadvantage by encompassing the LR model, decreasing the marginal cost of the error metrics. The statistical metrics for the preferred algorithms were computed using the prediction outcomes of every sample, as illustrated in Table 4. The correlation between the actual and predicted values is shown in Figure 5.

Table 4. Statistical metrics of ML model

Model	Testing Set				Training Set			
	RMSE	MAE	R^2	SMAPE	RMSE	MAE	R^2	SMAPE
XGBoost	44.3420	35.0929	0.9200	0.0396	39.1869	30.4126	0.9584	0.0330
LR	490.1090	478.6924	−8.7707	0.8437	510.0522	500.2727	−6.0547	0.8720
Final Model	48.5147	41.7175	0.9043	0.0484	40.9851	32.0309	0.9544	0.0344

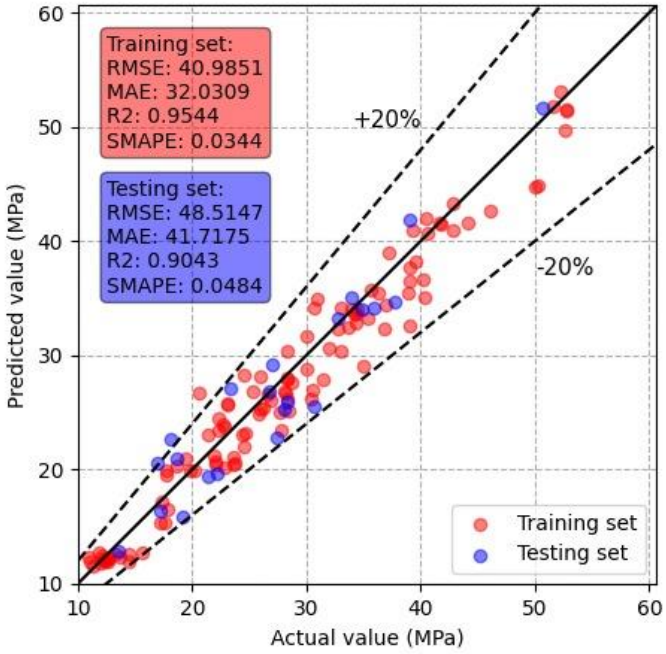

Figure 5. Relationship between actual and predicted values of compressive strength

The graph shows that most samples fall within a relative error range of 20%. This finding indicates that the predicted value can adequately describe the actual results even though it is not entirely precise. Sensitivity analysis was also performed to ascertain each variable's influence on the XGBoost model's prediction output, as shown in Figure 6. The age of the mixture is by far the most essential feature for the XGBoost model, followed by the least important feature, which is the mass of the coarse aggregate, with nearly 0% importance. However, feature importance does not indicate the effect of increasing or decreasing the value of a feature. It also neglects the impact of the LR model. We refer to the partial dependence plot shown in Figure 7.

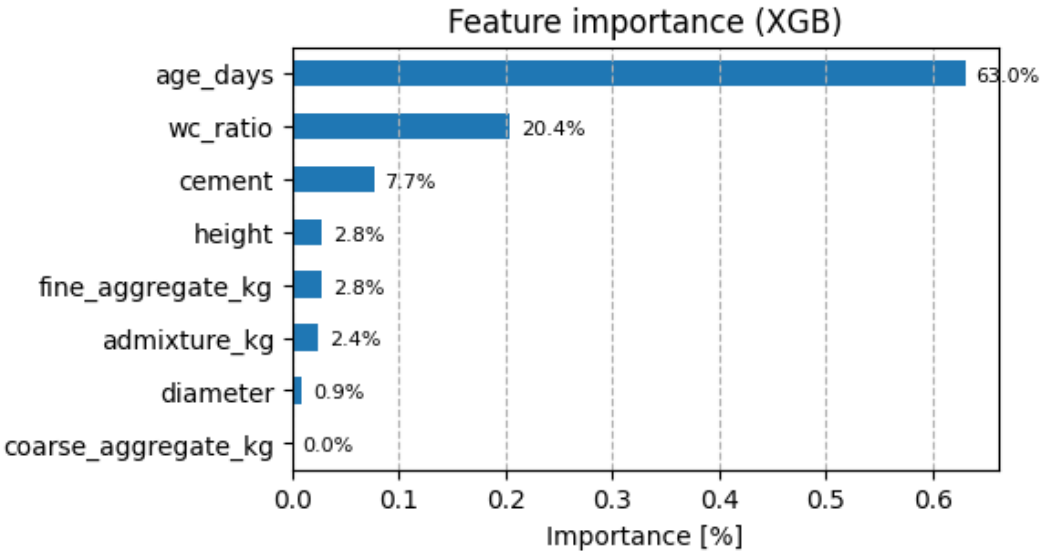

Figure 6. Feature importance outcomes derived from ML models

The partial dependence plot shows the effect of increasing or decreasing the value of a feature for the entire final model in the final equation. It reveals that while most features have less correlation to the predicted target, the age of the mixture has a strong positive correlation, and the water-cement ratio has a strong negative correlation. This is due to the strong weightage effect from the XGBoost model. The final prediction of a slump for a sample is expressed as follows:

$$f_{slump}(wcr, m_w, m_{ad}, \dots) = 57.34 \times wcr + 0.26 \times m_w + 0.96 \times m_{ad} + 3.79 \times \log(1 + m_{ad}) - 73.4 \quad (5)$$

The equation is found by training a linear regression model with the log feature of the mass of the admixture.

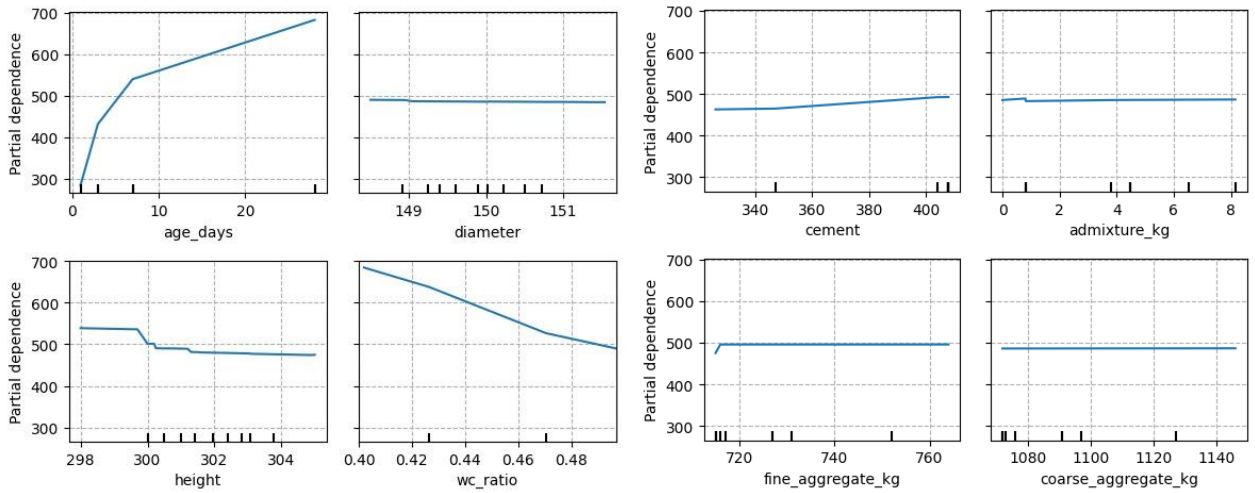

Figure 7. Partial dependence diagram of the variable input

The laboratory test findings indicate that scheme 3 offers enhanced performance while simultaneously decreasing the amount of cement needed. A predictive experiment was conducted utilizing a dataset within the range of scheme 3 to determine the maximum compressive strength that could be attained at the age of three days. In addition, the maximum possible reduction in carbon emissions must be determined. The carbon emission value is identified by calculating the embodied carbon using data from the Inventory of Carbon and Energy (ICE) 2019 database, without considering the waste factor [5, 86]. In concrete structure materials, embodied carbon has contributed up to 58.13% of the total carbon emissions compared to transportation, equipment, and electricity emissions [87].

The volume of each material is multiplied by its corresponding emission factor, which is calculated in the bill of quantities, to determine the amount of carbon contained in concrete. This approach allows us to express the embodied carbon in units of $kgCO_2/kg$ [88]. The cost of each material was determined through market research conducted at the research location region. The market price of each material is multiplied by its corresponding volume to calculate the production cost. Table 5 displays the parameter values for carbon emission factors and production costs. The result of compressive strength prediction alongside the cost and carbon parameters for the new dataset can be seen in Table 6.

The production costs of materials and embodied carbon are calculated using the following formula:

$$CE = m_w CE_w + m_c CE_c + m_{fa} CE_{fa} + m_{ca} CE_{ca} + m_{ad} CE_{ad} \quad (6)$$

$$PC = m_w PC_w + m_c PC_c + m_{fa} PC_{fa} + m_{ca} PC_{ca} + m_{ad} PC_{ad} \quad (7)$$

Table 5. Parameter for calculating carbon emission and production cost of concrete

Parameter		Units	Carbon Emission Factor (CE) [5]	Production Cost (PC)*	Production Cost (PC)	Density**
			$kgCO_2/kg$	IDR	USD	kg/m^3
Water content	*W*	kg	0.0003	10	0.0006	1000
Cement content	*c*	kg	0.9120	1,294	0.0809	3100
Fine aggregates	*fa*	kg	0.0075	150	0.0093	2687
Coarse aggregates	*ca*	kg	0.0075	275	0.0172	2630
Admixture	*ad*	kg	1.8800	45,000	2.8125	1170

* Obtained from market research

** Obtained from laboratory test

The prediction model was used to evaluate multiple schemes. The 5B scheme achieved the highest 3-day compressive strength, 29.18 MPa. By contrast, the 4D scheme had the lowest embodied carbon, 350.16 $kgCO_2/kg$. Nevertheless, production costs increased in all alternatives, necessitating optimization processes to achieve enhanced performance. Moreover, carbon emissions decreased, along with reduced production costs.

Table 6. Resulting in optimized compressive strength prediction results, production costs, and carbon emissions

Scheme	Age (days)	fc' (MPa)	Cost of Material		Embodied Carbon	
0	3	21.91	932,450	100.00%	385.44	100.00%
3A	3	24.09	965,255	103.52%	383.36	99.46%
4B	3	21.58	986,735	105.82%	370.50	96.12%
4C	3	21.53	1,009,960	108.31%	359.42	93.25%
4D	3	21.48	1,034,929	111.04%	350.16	90.84%
5A	3	27.81	988,908	106.04%	403.27	104.62%
5B	3	29.18	1,009,459	108.36%	390.40	101.29%
5C	3	27.93	1,031,861	110.73%	378.42	98.18%
5D	3	27.88	1,056,113	113.34%	368.25	95.54%
6A	3	27.89	988,194	106.09%	370.58	96.14%
6B	3	27.89	1,061,352	113.90%	368.42	95.58%

6. Multi-Objective Optimization

The original value must be ascertained to obtain the optimization value used as the benchmark. The control variable in this study was scheme 0 with a compressive strength of 30 Mpa, without using any admixture. The optimization outcomes are compared with the control variables to determine the extent of performance enhancement and cost reduction. The parameters used in PSO are presented in Table 7. The following formula is used to achieve optimization:

$$f(m_c, \ldots., m_{w)} = \alpha_1 \frac{|CS-CS^*|}{CS} + \alpha_2 \frac{|PC-PC^*|}{PC} + \alpha_3 \frac{|CE-CE^*|}{CE} + \alpha_4 \frac{|S-S^*|}{S}, \quad (8)$$

where CS, PC, CE, and S are the predicted compressive strength, production cost, carbon emission, and the predicted slump for a sample. The novelty in this study is that the weight of each parameter (α_1, α_2, α_3) is determined by analyzing the preferences of construction stakeholders in Indonesia using the AHP method. CS^*, PC^*, CE^*, and S^*represent the desired corresponding target depending on the scenario. The constraint is expressed as follows:

$$V_{tot} = \frac{m_c}{D_c} + \frac{m_w}{D_w} + \frac{m_{fa}}{D_{fa}} + \frac{m_{ca}}{D_{ca}} + \frac{m_{ad}}{D_{ad}} = 1. \quad (9)$$

The parameters used during the PSO process for all of the scenarios are as follows:

$c_1 = c_2 = 2.0$
$G_k = 50$
$w = 0.9$
Number of particles = 200

Table 7. Multi-objective optimization parameter target for PSO simulation

Scenario	α_1	α_2	α_3	α_4	Age (Days)	CS target	PC target	CE target	Slump range target
1	0.6333	0.2605	0.1062	-	28	29.18	932,450	350.155	-
2	0.6333	0.2605	0.1062	-	3	29.18	932,450	350.155	-
3	0.6333	0.2605	0.1062	-	3	21	932,450	350.155	-
4	0.6333	0.2605	0.1062	1.0000	28	30	932,450	350.155	8–12
5	0.6333	0.2605	0.1062	1.0000	3	28.18	932,450	350.155	8–12
6	0.6333	0.2605	0.1062	1.0000	3	21.91	932,450	350.155	8–12
7	0.5700	0.2345	0.0955	0.1000	28	30	932,450	350.155	8–12
8	0.5700	0.2345	0.0955	0.1000	3	28.18	932,450	350.155	8–12
9	0.5700	0.2345	0.0955	0.1000	3	21.91	932,450	350.155	8–12

α_1 = 63.33%, α_2 = 26.05%, α_3 = 10.62% [76].

The optimization target parameters are set, prompting ML to search for results that closely approximate these parameters. Two scenarios are applied to achieve two optimization alternatives. The first scenario utilizes the maximum three-day compressive strength parameters, the lowest production costs, and the lowest carbon emissions. The 3-day compressive strength is used because it can improve performance. In addition, construction could be accelerated. In the second scenario, the 3-day compressive strength characteristics remain unchanged from the standard scheme, with the lowest production costs and carbon emissions. Table 8. summarizes the simulation result and compares scheme 0 and the PSO output results regarding compressive strength, production costs, and embodied carbon.

Table 8 shows that the value of the embodied carbon decreases in all scenarios that result from optimization using PSO. Nevertheless, not all individuals benefited from price reductions. As a result of the absence of slump as an input parameter in the PSO in scenarios 1 and 2, the obtained slump values cannot sufficiently satisfy the technical requirements of 10 ± 2 cm. In scenario 3, the cost efficiency and reduction in embodied carbon are relatively satisfactory, but the compressive strength experiences a slight decrease. Cost and carbon emission reductions are highly dependent on the composition of cement and admixture. The study results showed that the reductions were consistent as long as the additional costs and carbon emissions due to adding admixture were not more significant than the reductions in costs and carbon emissions due to reducing cement volume. The engineer may re-analyze the actual compressive strength value to ascertain the structure's overall capacity in line with this 1–2 MPa reduction. This reduction should not significantly impact the efficacy of the structure. Referring to ACI 347.2R-17, the determination of concrete strength is essential for the timely removal of formwork, affected by the pace of strength development, the accuracy of strength assessment, and the load and deformation capacity of the structure. The optimization findings indicate that all models show compressive strength values surpassing 70% at 3 days of age. The material has met the minimum requirements for structural load-bearing as designed [89]. It suggests that this optimization method can accelerate the removal of formwork and shoring in concrete structures.

Scenarios 3, 4, and 7 were selected for validation through laboratory testing in the subsequent stage. Scenarios 3 and 7 were applied because the reduction in embodied carbon value and production costs were the most significant (9.12%–10.41% carbon reduction; 0.79%–3.06% cost reduction). Meanwhile, scenario 4 was preferred because the increase in compressive strength is relatively high (29.16%), but the costs and embodied carbon decrease significantly (8.13% carbon reduction and 0.97% cost reduction). However, in scenario 4, the slump value is minimal. Therefore, mixing tests were carried out using delayed and immediate addition of admixture [75]. Compared to other studies, material optimization using various techniques (including machine learning) can lead to up to 40% cost efficiency and 2.63%–60% greenhouse gas reduction potential in construction projects. In this study, the optimization can lead to carbon reduction by 7%—10% and cost reduction by 1%—3% for each m³ of concrete. Combining with early removal of formwork and shoring, it may lead to a 20%-30% cost reduction in building construction projects, which need to be studied further.

7. Model Validation

To validate the mathematical model, laboratory testing was performed again using the mixed design composition of the PSO output results. Table 9 displays the outcomes of this laboratory validation. The average deviation of all tests is only 2,515 MPa, which is not greater than 15%. Because the actual compressive strength value as a divider is still relatively small at the age of one day, the relative error is substantial, but it is still below 20%. This finding demonstrates that the compressive strength prediction value generated by the ML algorithm closely approximates the actual compressive strength results. The compressive strength value predicted by the ML is greater than the actual compressive strength in schemes 0, 4, and 7, except for 28 days in scheme 7. Because of limited training data, some ML predictions may deviate significantly from expectations. While in the results of laboratory evidence, sometimes there are factors that slightly affect the results of concrete compressive strength to be different, including curing conditions, test age not the same (a difference of several hours), non-uniformity of aggregate material, and other factors that need to be studied further. The overall results of schemes 3, 4, and 7 suggest that a solution was obtained, satisfying the technical requirements and reducing production costs and the embodied carbon.

Regarding the slump, a validation test was also conducted immediately with the addition of admixture and with a delay. The results of the slump test and slump loss validation tests are shown in Figure 8. The result indicates that delayed admixture addition can impact slump remarkably, contrary to the effect of immediate addition of admixture. Scenario 4, with delayed admixture addition, demonstrates a substantial slump increment (78%), whereas scenarios 3 and 7, with delayed admixture, show increases of only 30 and 39%, respectively. The slump prediction result did not achieve satisfactory accuracy because of limitations in the dataset. A broad range of objective slump data is required to improve slump value predictions beyond the available data of the current study.

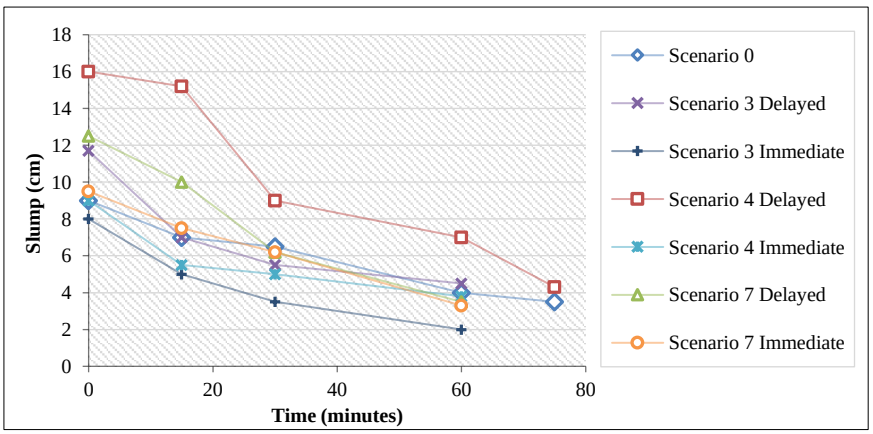

Figure 8. Concrete slump comparison among scenarios 0, 3, 4, and 7 for immediate and delayed conditions

Table 8. Concrete design mix optimization using PSO considering compressive strength, costs, and carbon emissions

Scenario	Age (days)	PSO Results								Compressive Strength, Cost, Embodied Carbon, and Slump Comparison						
		CS result (MPa)	PC result (IDR)	CE result ($kgCO_2$)	Slump Result (cm)	Water (L)	Cement (kg)	Fine aggregate (kg)	Coarse aggregate (kg)	Admixture (L)	fc' 3 days (MPa)	fc' 28 days (MPa)	Embodied Carbon Deviation ($kgCO_2$)		Production Cost Deviation (IDR)		Slump
0											21.91	30.56	385.44	0.00	932,450	0	10
1	28	39.59	928,660	358.47	-	185.7	376.97	718.27	1127.33	0.47	27.64	39.59	358.47	−26.97	928,660	−3,790	4.96
2	3	27.87	934,961	359.16	-	178.77	377.44	743.85	1129.42	0.5	27.87	39.82	359.16	−26.28	934,961	2,511	2.18
3	3	21.01	925,122	350.3	-	193.92	367.43	746.7	1092.85	0.78	21.01	28.99	350.3	−35.14	925,122	−7,328	9.89
4	28	39.47	923,419	354.11	5.33	186.32	372.18	726.99	1137.49	0.4	24.42	39.47	354.11	−31.33	923,419	−9,031	5.33
5	3	24.51	947,221	367.87	8.08	193.14	386.86	738.77	1097.55	0.71	24.51	39.55	367.87	−17.57	947,221	14,771	8.08
6	3	27.56	970,918	365.75	8.12	188.66	383.29	737.76	1109.6	1.27	27.56	40.43	365.75	−19.69	970,918	38,468	8.12
7	28	29	903,932	345.32	7.58	190.59	363.82	720.55	1122.22	0.35	21.02	29	345.32	−40.12	903,932	−28,518	7.58
8	3	27.66	983,144	373.28	8.87	191.16	392.42	728.85	1096.02	1.42	27.66	40.54	373.28	−12.16	983,144	50,694	8.87
9	3	27.56	970,918	365.75	8.12	188.66	383.29	737.76	1109.6	1.27	27.56	40.43	365.75	−19.69	970,918	38,468	8.12

Table 9. Comparison of the compressive strength results from the laboratory test validation and the predicted results

Scenario	Curing age (days)	Actual fc' (MPa)	Prediction fc'(MPa)	Deviation (MPa)	Relative Error (%)
0	1	10.982	13.050	2.068	18.83%
0	3	20.714	21.820	1.106	5.34%
0	7	27.126	28.110	0.984	3.63%
0	28	34.688	35.760	1.072	3.09%
3	1	14.092	12.920	−1.172	8.32%
3	3	24.599	21.010	−3.589	14.59%
3	7	28.261	26.060	−2.201	7.79%
3	28	35.956	29.000	−6.956	19.35%
4	1	14.325	16.050	1.725	12.04%
4	3	20.892	24.420	3.528	16.89%
4	7	26.733	29.530	2.797	10.46%
4	28	37.500	39.470	1.970	5.25%
7	1	11.448	12.900	1.452	12.68%
7	3	20.153	21.020	0.867	4.30%
7	7	24.269	26.040	1.771	7.30%
7	28	32.797	28.980	−3.817	11.64%
Absolute Average				**2.515**	**11.10%**

8. Conclusion

The construction industry is seeking sustainable concrete solutions without compromising cost. This study presents an innovative method for predicting the optimum mix design without compromising carbon emissions or production costs. It uses XGBoost and LR algorithms to model concrete compressive strength at specific ages and an optimization framework called PSO to derive a mix composition that meets compressive strength standards, reduces emissions, and minimizes production costs. The PSO weight parameter has been derived from stakeholder preference analysis of construction in Indonesia with the AHP method. The XGBoost and LR model combination achieved an R^2 of 0.9043, an RMSE of 48.5147, and a MAPE of 0.0484, indicating that the compressive strength of concrete is most significantly influenced by its age, wc ratio, and cement composition. Minimizing the required cement can reduce carbon content by 7%—10% and slightly decrease production costs by 1%—3%. Combining with early removal of formwork and shoring, it may lead to a 20%-30% cost reduction in building construction projects, which need to be studied further.

Laboratory testing was conducted to validate the result of PSO simulation, achieving a relative error of 11.10%. This finding demonstrates that the compressive strength prediction value generated by the ML algorithm closely approximates the actual compressive strength results. Regarding the slump prediction, the validation still does not meet the expectation due to limited data. A further study using more data, including the immediate and delayed admixture addition technique, shall be conducted. The study findings reveal that optimizing the concrete design mix in construction projects in Indonesia can significantly reduce carbon emissions. Applying this strategy to all projects could reduce global emissions by 4 million metric tons of CO2. These findings are crucial for concrete manufacturers and builders seeking cost and carbon emission savings in sustainable concrete mix designs. In further research, the results of this study can be simulated and analyzed using lifecycle analysis to determine carbon reduction and construction project costs in an ongoing project cycle.

9. Declarations

9.1. Author Contributions

Conceptualization, A.T.Y., A.S.B.N., I.S., and M.S.; methodology, A.T.Y., A.S.B.N., I.S., and T.N.H.; formal analysis, A.T.Y. and R.E.; investigation, A.T.Y., A.R.E., and J.L.; data curation, A.T.Y., A.R.E., and J.L.; writing—original draft preparation, A.T.Y. and R.E.; writing—review and editing, A.S.B.N., I.S., T.N.H., and M.S.; visualization, R.E.; supervision, A.S.B.N. and I.S.; funding acquisition, A.S.B.N. All authors have read and agreed to the published version of the manuscript.

9.2. Data Availability Statement

The data presented in this study are available on request from the corresponding author.

9.3. Funding and Acknowledgments

The authors gratefully acknowledge the financial support from the Final Assignment Recognition Program of the University of Gadjah Mada no. 5286/UN1.P1/PT.01.03/2024.

9.4. Institutional Review Board Statement

Not applicable.

9.5. Informed Consent Statement

Not applicable.

9.6. Declaration of Competing Interest

The authors declare that there are no conflicts of interest concerning the publication of this manuscript. Furthermore, all ethical considerations, including plagiarism, informed consent, misconduct, data fabrication and/or falsification, double publication and/or submission, and redundancies have been completely observed by the authors.

10. References

[1] Yu, M., Robati, M., Oldfield, P., Wiedmann, T., Crawford, R., Nezhad, A. A., & Carmichael, D. (2020). The impact of value engineering on embodied greenhouse gas emissions in the built environment: A hybrid life cycle assessment. Building and Environment, 168(10), 106452. doi:10.1016/j.buildenv.2019.106452.

[2] Belizario-Silva, F., Costa Reis, D., Carvalho, M., Leopoldo e Silva França, R., & John, V. M. (2024). Material intensity and embodied CO2 benchmark for reinforced concrete structures in Brazil. Journal of Building Engineering, 82, 108234. doi:10.1016/j.jobe.2023.108234.

[3] Dong, Y. H., Jaillon, L., Chu, P., & Poon, C. S. (2015). Comparing carbon emissions of precast and cast-in-situ construction methods - A case study of high-rise private building. Construction and Building Materials, 99, 39–53. doi:10.1016/j.conbuildmat.2015.08.145.

[4] Mehta, V. (2023). Machine learning approach for predicting concrete compressive, splitting tensile, and flexural strength with waste foundry sand. Journal of Building Engineering, 70(January), 106363. doi:10.1016/j.jobe.2023.106363.

[5] Hammond, G., Jones, C., Lowrie, F., & Tse, P. (2008). Inventory of Carbon & Energy: ICE: Sustainable Energy Research Team. Department of Mechanical Engineering, University of Bath, Bath, England.

[6] Mancke, R., Stephan, D., & Firdous, R. (2024). Case study - Sustainable concrete development: Assessing social, environmental, and performance factors of geopolymers and CEM-I concretes. Case Studies in Construction Materials, 21(July), 3448. doi:10.1016/j.cscm.2024.e03448.

[7] McLellan, B. C., Williams, R. P., Lay, J., Van Riessen, A., & Corder, G. D. (2011). Costs and carbon emissions for geopolymer pastes in comparison to ordinary portland cement. Journal of Cleaner Production, 19(9–10), 1080–1090. doi:10.1016/j.jclepro.2011.02.010.

[8] Sandanayake, M., Gunasekara, C., Law, D., Zhang, G., Setunge, S., & Wanijuru, D. (2020). Sustainable criterion selection framework for green building materials – An optimisation based study of fly-ash Geopolymer concrete. Sustainable Materials and Technologies, 25, 178. doi:10.1016/j.susmat.2020.e00178.

[9] Thilakarathna, P. S. M., Seo, S., Baduge, K. S. K., Lee, H., Mendis, P., & Foliente, G. (2020). Embodied carbon analysis and benchmarking emissions of high and ultra-high strength concrete using machine learning algorithms. Journal of Cleaner Production, 262(February), 121281. doi:10.1016/j.jclepro.2020.121281.

[10] Chi, L., Wang, M., Liu, K., Lu, S., Kan, L., Xia, X., & Huang, C. (2023). Machine learning prediction of compressive strength of concrete with resistivity modification. Materials Today Communications, 36(3), 106470. doi:10.1016/j.mtcomm.2023.106470.

[11] Chakraborty, D., Awolusi, I., & Gutierrez, L. (2021). An explainable machine learning model to predict and elucidate the compressive behavior of high-performance concrete. Results in Engineering, 11. doi:10.1016/j.rineng.2021.100245.

[12] Shahrokhishahraki, M., Malekpour, M., Mirvalad, S., & Faraone, G. (2024). Machine learning predictions for optimal cement content in sustainable concrete constructions. Journal of Building Engineering, 82. doi:10.1016/j.jobe.2023.108160.

[13] Li, Y., Shen, J., Lin, H., & Li, Y. (2023). Optimization design for alkali-activated slag-fly ash geopolymer concrete based on artificial intelligence considering compressive strength, cost, and carbon emission. Journal of Building Engineering, 75(100), 106929. doi:10.1016/j.jobe.2023.106929.

[14] Kim, T., Tae, S., & Roh, S. (2013). Assessment of the CO2 emission and cost reduction performance of a low-carbon-emission concrete mix design using an optimal mix design system. Renewable and Sustainable Energy Reviews, 25, 729–741. doi:10.1016/j.rser.2013.05.013.

[15] Tavares, C., & Grasley, Z. (2022). Machine learning-based mix design tools to minimize carbon footprint and cost of UHPC. Part 2: Cost and eco-efficiency density diagrams. Cleaner Materials, 4(May), 100094. doi:10.1016/j.clema.2022.100094.

[16] Alabi, S. A., Arum, C., Adewuyi, A. P., Arum, R. C., Afolayan, J. O., & Mahachi, J. (2023). Mathematical model for prediction of compressive strength of ternary blended cement concrete utilizing gene expression programming. Scientific African, 22(October), 1954. doi:10.1016/j.sciaf.2023.e01954.

[17] Md Akram Hossain, Islam, G. M. S., & Amit Mallick. (2022). Compressive Strength Prediction for Industrial Waste-Based SCC Using Artificial Neural Network. Journal of the Civil Engineering Forum, 9(January), 11–26. doi:10.22146/jcef.4094.

[18] Duan, J., Asteris, P. G., Nguyen, H., Bui, X. N., & Moayedi, H. (2021). A novel artificial intelligence technique to predict compressive strength of recycled aggregate concrete using ICA-XGBoost model. Engineering with Computers, 37(4), 3329–3346. doi:10.1007/s00366-020-01003-0.

[19] Shah, S. F. A., Chen, B., Zahid, M., & Ahmad, M. R. (2022). Compressive strength prediction of one-part alkali activated material enabled by interpretable machine learning. Construction and Building Materials, 360(July), 129534. doi:10.1016/j.conbuildmat.2022.129534.

[20] Mai, H. V. T., Nguyen, M. H., & Ly, H. B. (2023). Development of machine learning methods to predict the compressive strength of fiber-reinforced self-compacting concrete and sensitivity analysis. Construction and Building Materials, 367 (January), 130339. doi:10.1016/j.conbuildmat.2023.130339.

[21] Li, Y., Li, H., jin, C., & Shen, J. (2022). The study of effect of carbon nanotubes on the compressive strength of cement-based materials based on machine learning. Construction and Building Materials, 358(July), 129435. doi:10.1016/j.conbuildmat.2022.129435.

[22] Wang, S., Xia, P., Gong, F., Zeng, Q., Chen, K., & Zhao, Y. (2024). Multi objective optimization of recycled aggregate concrete based on explainable machine learning. Journal of Cleaner Production, 445(January), 141045. doi:10.1016/j.jclepro.2024.141045.

[23] Winarno, S., & Kusumadewi, S. (2024). Application of Soft Computing to Address Uncertainty in Construction Project Management: A Systematic Literature Review. Civil Engineering Journal, 10(6), 2040-2065. doi:10.28991/CEJ-2024-010-06-020.

[24] Taffese, W. Z., & Espinosa-Leal, L. (2023). Multitarget regression models for predicting compressive strength and chloride resistance of concrete. Journal of Building Engineering, 72. doi:10.1016/j.jobe.2023.106523.

[25] Ekanayake, I. U., Meddage, D. P. P., & Rathnayake, U. (2022). A novel approach to explain the black-box nature of machine learning in compressive strength predictions of concrete using Shapley additive explanations (SHAP). Case Studies in Construction Materials, 16(April), 1059. doi:10.1016/j.cscm.2022.e01059.

[26] Cao, C. (2023). Prediction of concrete porosity using machine learning. Results in Engineering, 17(August), 100794. doi:10.1016/j.rineng.2022.100794.

[27] Yang, J., Zeng, B., Ni, Z., Fan, Y., Hang, Z., Wang, Y., Feng, C., & Yang, J. (2023). Comparison of traditional and automated machine learning approaches in predicting the compressive strength of graphene oxide/cement composites. Construction and Building Materials, 394(March), 132179. doi:10.1016/j.conbuildmat.2023.132179.

[28] Balasooriya Arachchilage, C., Huang, G., Fan, C., & Liu, W. V. (2023). Forecasting unconfined compressive strength of calcium sulfoaluminate cement mixtures using ensemble machine learning techniques integrated with shapely-additive explanations. Construction and Building Materials, 409(October), 134083. doi:10.1016/j.conbuildmat.2023.134083.

[29] Li, Q., & Song, Z. (2023). Prediction of compressive strength of rice husk ash concrete based on stacking ensemble learning model. Journal of Cleaner Production, 382(November 2022), 135279. doi:10.1016/j.jclepro.2022.135279.

[30] Munir, M. J., Kazmi, S. M. S., Wu, Y. F., Lin, X., & Ahmad, M. R. (2022). Development of novel design strength model for sustainable concrete columns: A new machine learning-based approach. Journal of Cleaner Production, 357(April), 131988. doi:10.1016/j.jclepro.2022.131988.

[31] Liu, K., Zhang, L., Wang, W., Zhang, G., Xu, L., Fan, D., & Yu, R. (2023). Development of compressive strength prediction platform for concrete materials based on machine learning techniques. Journal of Building Engineering, 80(July), 107977. doi:10.1016/j.jobe.2023.107977.

[32] Zhang, T., Zhang, Y., Wang, Q., Aganyira, A. K., & Fang, Y. (2023). Experimental study and machine learning prediction on compressive strength of spontaneous-combustion coal gangue aggregate concrete. Journal of Building Engineering, 71(January), 106518. doi:10.1016/j.jobe.2023.106518.

[33] Alyami, M., Nassar, R. U. D., Khan, M., Hammad, A. W., Alabduljabbar, H., Nawaz, R., Fawad, M., & Gamil, Y. (2024). Estimating compressive strength of concrete containing rice husk ash using interpretable machine learning-based models. Case Studies in Construction Materials, 20, 2901. doi:10.1016/j.cscm.2024.e02901.

[34] Kashem, A., Karim, R., Das, P., Datta, S. D., & Alharthai, M. (2024). Compressive strength prediction of sustainable concrete incorporating rice husk ash (RHA) using hybrid machine learning algorithms and parametric analyses. Case Studies in Construction Materials, 20(March), 3030. doi:10.1016/j.cscm.2024.e03030.

[35] Liu, G., & Sun, B. (2023). Concrete compressive strength prediction using an explainable boosting machine model. Case Studies in Construction Materials, 18(October 2022), 1845. doi:10.1016/j.cscm.2023.e01845.

[36] Li, H., Lin, J., Zhao, D., Shi, G., Wu, H., Wei, T., Li, D., & Zhang, J. (2022). A BFRC compressive strength prediction method via kernel extreme learning machine-genetic algorithm. Construction and Building Materials, 344(April), 128076. doi:10.1016/j.conbuildmat.2022.128076.

[37] Montazerian, A., Baghban, M. H., Ramachandra, R., & Goutianos, S. (2023). A machine learning approach for assessing the compressive strength of cementitious composites reinforced by graphene derivatives. Construction and Building Materials, 409(January), 134014. doi:10.1016/j.conbuildmat.2023.134014.

[38] Kellouche, Y., Tayeh, B. A., Chetbani, Y., Zeyad, A. M., & Mostafa, S. A. (2024). Comparative study of different machine learning approaches for predicting the compressive strength of palm fuel ash concrete. Journal of Building Engineering, 88(April), 109187. doi:10.1016/j.jobe.2024.109187.

[39] Alavi, S. A., Noel, M., Moradi, F., & Layssi, H. (2024). Development of a machine learning model for on-site evaluation of concrete compressive strength by SonReb. Journal of Building Engineering, 82, 108328. doi:10.1016/j.jobe.2023.108328.

[40] Karim, R., Islam, M. H., Datta, S. D., & Kashem, A. (2024). Synergistic effects of supplementary cementitious materials and compressive strength prediction of concrete using machine learning algorithms with SHAP and PDP analyses. Case Studies in Construction Materials, 20(November), 2828. doi:10.1016/j.cscm.2023.e02828.

[41] Günaydın, O., Akbaş, E., Özbeyaz, A., & Güçlüer, K. (2023). Machine learning based evaluation of concrete strength from saturated to dry by non-destructive methods. Journal of Building Engineering, 76. doi:10.1016/j.jobe.2023.107174.

[42] Wu, Y., & Zhou, Y. (2022). Hybrid machine learning model and Shapley additive explanations for compressive strength of sustainable concrete. Construction and Building Materials, 330(March), 127298. doi:10.1016/j.conbuildmat.2022.127298.

[43] Rathnayaka, M., Karunasinghe, D., Gunasekara, C., Wijesundara, K., Lokuge, W., & Law, D. W. (2024). Machine learning approaches to predict compressive strength of fly ash-based geopolymer concrete: A comprehensive review. Construction and Building Materials, 419, 135519. doi:10.1016/j.conbuildmat.2024.135519.

[44] Ding, Y., Wei, W., Wang, J., Wang, Y., Shi, Y., & Mei, Z. (2023). Prediction of compressive strength and feature importance analysis of solid waste alkali-activated cementitious materials based on machine learning. Construction and Building Materials, 407(July), 133545. doi:10.1016/j.conbuildmat.2023.133545.

[45] Shen, J., Li, Y., Lin, H., Li, H., Lv, J., Feng, S., & Ci, J. (2022). Prediction of compressive strength of alkali-activated construction demolition waste geopolymers using ensemble machine learning. Construction and Building Materials, 360(100), 129600. doi:10.1016/j.conbuildmat.2022.129600.

[46] Huo, W., Zhu, Z., Sun, H., Ma, B., & Yang, L. (2022). Development of machine learning models for the prediction of the compressive strength of calcium-based geopolymers. Journal of Cleaner Production, 380(P2), 135159. doi:10.1016/j.jclepro.2022.135159.

[47] Eftekhar Afzali, S. A., Shayanfar, M. A., Ghanooni-Bagha, M., Golafshani, E., & Ngo, T. (2024). The use of machine learning techniques to investigate the properties of metakaolin-based geopolymer concrete. Journal of Cleaner Production, 446(February), 141305. doi:10.1016/j.jclepro.2024.141305.

[48] Parhi, S. K., & Patro, S. K. (2023). Prediction of compressive strength of geopolymer concrete using a hybrid ensemble of grey wolf optimized machine learning estimators. Journal of Building Engineering, 71(March), 106521. doi:10.1016/j.jobe.2023.106521.

[49] Wang, Y., Iqtidar, A., Amin, M. N., Nazar, S., Hassan, A. M., & Ali, M. (2024). Predictive modelling of compressive strength of fly ash and ground granulated blast furnace slag based geopolymer concrete using machine learning techniques. Case Studies in Construction Materials, 20, 3130. doi:10.1016/j.cscm.2024.e03130.

[50] Ahmad, A., Ahmad, W., Aslam, F., & Joyklad, P. (2022). Compressive strength prediction of fly ash-based geopolymer concrete via advanced machine learning techniques. Case Studies in Construction Materials, 16, 840. doi:10.1016/j.cscm.2021.e00840.

[51] Pal, A., Ahmed, K. S., Hossain, F. Z., & Alam, M. S. (2023). Machine learning models for predicting compressive strength of fiber-reinforced concrete containing waste rubber and recycled aggregate. Journal of Cleaner Production, 423(May), 138673. doi:10.1016/j.jclepro.2023.138673.

[52] Liu, K., Zheng, J., Dong, S., Xie, W., & Zhang, X. (2023). Mixture optimization of mechanical, economical, and environmental objectives for sustainable recycled aggregate concrete based on machine learning and metaheuristic algorithms. Journal of Building Engineering, 63. doi:10.1016/j.jobe.2022.105570.

[53] Yang, S., Sun, J., & Zhifeng, X. (2024). Prediction on compressive strength of recycled aggregate self-compacting concrete by machine learning method. Journal of Building Engineering, 88. doi:10.1016/j.jobe.2024.109055.

[54] Quan Tran, V., Quoc Dang, V., & Si Ho, L. (2022). Evaluating compressive strength of concrete made with recycled concrete aggregates using machine learning approach. Construction and Building Materials, 323(January), 126578. doi:10.1016/j.conbuildmat.2022.126578.

[55] Huang, P., Dai, K., & Yu, X. (2023). Machine learning approach for investigating compressive strength of self-compacting concrete containing supplementary cementitious materials and recycled aggregate. Journal of Building Engineering, 79(July), 107904. doi:10.1016/j.jobe.2023.107904.

[56] Mahmood, M. S., Elahi, A., Zaid, O., Alashker, Y., Şerbănoiu, A. A., Grădinaru, C. M., Ullah, K., & Ali, T. (2023). Enhancing compressive strength prediction in self-compacting concrete using machine learning and deep learning techniques with incorporation of rice husk ash and marble powder. Case Studies in Construction Materials, 19(September), e02557. doi:10.1016/j.cscm.2023.e02557.

[57] de-Prado-Gil, J., Palencia, C., Silva-Monteiro, N., & Martínez-García, R. (2022). To predict the compressive strength of self compacting concrete with recycled aggregates utilizing ensemble machine learning models. Case Studies in Construction Materials, 16(April), 1046. doi:10.1016/j.cscm.2022.e01046.

[58] Yuan, Y., Yang, M., Shang, X., Xiong, Y., & Zhang, Y. (2023). Predicting the compressive strength of UHPC with coarse aggregates in the context of machine learning. Case Studies in Construction Materials, 19(August), 2627. doi:10.1016/j.cscm.2023.e02627.

[59] Nagaraju, T. V., Mantena, S., Azab, M., Alisha, S. S., El Hachem, C., Adamu, M., & Rama Murthy, P. S. (2023). Prediction of high strength ternary blended concrete containing different silica proportions using machine learning approaches. Results in Engineering, 17(February), 100973. doi:10.1016/j.rineng.2023.100973.

[60] Das, P., & Kashem, A. (2024). Hybrid machine learning approach to prediction of the compressive and flexural strengths of UHPC and parametric analysis with shapley additive explanations. Case Studies in Construction Materials, 20(August), 2723. doi:10.1016/j.cscm.2023.e02723.

[61] Zhang, J., Niu, W., Yang, Y., Hou, D., & Dong, B. (2022). Machine learning prediction models for compressive strength of calcined sludge-cement composites. Construction and Building Materials, 346(July), 128442. doi:10.1016/j.conbuildmat.2022.128442.

[62] El Khessaimi, Y., El Hafiane, Y., Smith, A., Peyratout, C., Tamine, K., Adly, S., & Barkatou, M. (2023). Machine learning-based prediction of compressive strength for limestone calcined clay cements. Journal of Building Engineering, 76(March), 1–25. doi:10.1016/j.jobe.2023.107062.

[63] Alyami, M., Khan, M., Fawad, M., Nawaz, R., Hammad, A. W. A., Najeh, T., & Gamil, Y. (2024). Predictive modeling for compressive strength of 3D printed fiber-reinforced concrete using machine learning algorithms. Case Studies in Construction Materials, 20, 2728. doi:10.1016/j.cscm.2023.e02728.

[64] Alyousef, R., Rehman, M. F., Khan, M., Fawad, M., Khan, A. U., Hassan, A. M., & Ghamry, N. A. (2023). Machine learning-driven predictive models for compressive strength of steel fiber reinforced concrete subjected to high temperatures. Case Studies in Construction Materials, 19(June), 2418. doi:10.1016/j.cscm.2023.e02418.

[65] Sun, Y., & Lee, H. S. (2024). An interpretable probabilistic machine learning model for forecasting compressive strength of oil palm shell-based lightweight aggregate concrete containing fly ash or silica fume. Construction and Building Materials, 426(February), 136176. doi:10.1016/j.conbuildmat.2024.136176.

[66] Çalışkan, A., Demirhan, S., & Tekin, R. (2022). Comparison of different machine learning methods for estimating compressive strength of mortars. Construction and Building Materials, 335. doi:10.1016/j.conbuildmat.2022.127490.

[67] Khan, M. I., & Abbas, Y. M. (2023). Intelligent data-driven compressive strength prediction and optimization of reactive powder concrete using multiple ensemble-based machine learning approach. Construction and Building Materials, 404(August), 133148. doi:10.1016/j.conbuildmat.2023.133148.

[68] Maherian, M. F., Baran, S., Bicakci, S. N., Toreyin, B. U., & Atahan, H. N. (2023). Machine learning-based compressive strength estimation in nano silica-modified concrete. Construction and Building Materials, 408(October), 133684. doi:10.1016/j.conbuildmat.2023.133684.

[69] Luo, X., Li, Y., Lin, H., Li, H., Shen, J., Pan, B., Bi, W., & Zhang, W. (2023). Research on predicting compressive strength of magnesium silicate hydrate cement based on machine learning. Construction and Building Materials, 406(July), 133412. doi:10.1016/j.conbuildmat.2023.133412.

[70] Khan, M. A., Aslam, F., Javed, M. F., Alabduljabbar, H., & Deifalla, A. F. (2022). New prediction models for the compressive strength and dry-thermal conductivity of bio-composites using novel machine learning algorithms. Journal of Cleaner Production, 350(August), 131364. doi:10.1016/j.jclepro.2022.131364.

[71] Mahjoubi, S., Barhemat, R., Guo, P., Meng, W., & Bao, Y. (2021). Prediction and multi-objective optimization of mechanical, economical, and environmental properties for strain-hardening cementitious composites (SHCC) based on automated machine learning and metaheuristic algorithms. Journal of Cleaner Production, 329(August), 129665. doi:10.1016/j.jclepro.2021.129665.

[72] Sun, Z., Li, Y., Li, Y., Su, L., & He, W. (2024). Investigation on compressive strength of coral aggregate concrete: Hybrid machine learning models and experimental validation. Journal of Building Engineering, 82(December), 108220. doi:10.1016/j.jobe.2023.108220.

[73] Han, S. H., Khayat, K. H., Park, S., & Yoon, J. (2024). Machine learning-based approach for optimizing mixture proportion of recycled plastic aggregate concrete considering compressive strength, dry density, and production cost. Journal of Building Engineering, 83, 108393. doi:10.1016/j.jobe.2023.108393.

[74] Luo, X., Li, Y., Wang, Q., Mu, J., & Liu, Y. (2024). Machine learning based modeling for predicting the compressive strength of solid waste material-incorporated Magnesium Phosphate Cement. Journal of Cleaner Production, 442(January), 141172. doi:10.1016/j.jclepro.2024.141172.

[75] Collepardi, M. (1998). Admixtures used to enhance placing characteristics of concrete. Cement and Concrete Composites, 20(2–3), 103–112. doi:10.1016/s0958-9465(98)00071-7.

[76] Yudhistira, A. T., Nugroho, A. S. B., Satyarno, I., and T. N. Handayani. (2024). Analyzing Construction Stakeholder Perceptions in Indonesia: Analytic Hierarchy Process Approach for Quality, Cost, and Carbon Emission Assessment, 1-12.

[77] Xi, B., Zhang, N., Duan, H., He, J., Song, G., Li, H., & Shi, X. (2023). Optimization of rice husk ash concrete design towards economic and environmental assessment. Environmental Impact Assessment Review, 103(5), 107229. doi:10.1016/j.eiar.2023.107229.

[78] Chen, T., & Guestrin, C. (2016). XGBoost: A scalable tree boosting system. Proceedings of the ACM SIGKDD International Conference on Knowledge Discovery and Data Mining, 13-17-August-2016, 785–794. doi:10.1145/2939672.2939785.

[79] Kennedy, J., & Eberhart, R. (1995). Particle swarm optimization. Proceedings of ICNN'95-international Conference on Neural Networks, 4, 1942-1948. doi:10.1109/ICNN.1995.488968.

[80] Shi, Y., & Eberhart, R. (1998). A modified particle swarm optimizer. IEEE international conference on evolutionary computation proceedings. IEEE world congress on computational intelligence (Cat. No. 98TH8360), 69-73. doi:10.1109/ICEC.1998.699146.

[81] Clerc, M., & Kennedy, J. (2002). The particle swarm-explosion, stability, and convergence in a multidimensional complex space. IEEE Transactions on Evolutionary Computation, 6(1), 58–73. doi:10.1109/4235.985692.

[82] Pristyanto, Y., Mukarabiman, Z., & Nugraha, A. F. (2023). Extreme Gradient Boosting Algorithm to Improve Machine Learning Model Performance on Multiclass Imbalanced Dataset. International Journal on Informatics Visualization, 7(3), 710–715. doi:10.30630/joiv.7.3.1102.

[83] Poli, R., Kennedy, J., & Blackwell, T. (2007). Quantification & Assessment of the chemical form of residual gadolinium in the brain.pdf. Swarm Intell, 1, 33–57. doi:10.1007/s11721-007-0002-0.

[84] Engelbrecht, A. P. (2007). Computational intelligence: an introduction. John Wiley & Sons, New York, United States.

[85] Akiba, T., Sano, S., Yanase, T., Ohta, T., & Koyama, M. (2019). Optuna: A Next-generation Hyperparameter Optimization Framework. Proceedings of the ACM SIGKDD International Conference on Knowledge Discovery and Data Mining, 2623–2631. doi:10.1145/3292500.3330701.

[86] Jones, C. (2024). ICE Database - Embodied Carbon Model of Cement, Mortar and Concrete V1.2. Circular Ecology. Available online: https://circularecology.com/embodied-carbon-footprint-database.html (accessed on May 2024).

[87] Sandanayake, M., Lokuge, W., Zhang, G., Setunge, S., & Thushar, Q. (2018). Greenhouse gas emissions during timber and concrete building construction —A scenario based comparative case study. Sustainable Cities and Society, 38(8), 91–97. doi:10.1016/j.scs.2017.12.017.

[88] Sandanayake, M., Zhang, G., Setunge, S., Luo, W., & Li, C. Q. (2017). Estimation and comparison of environmental emissions and impacts at foundation and structure construction stages of a building – A case study. Journal of Cleaner Production, 151, 319–329. doi:10.1016/j.jclepro.2017.03.041.

[89] Skibicki, S. (2017). Optimization of Cost of Building with Concrete Slabs Based on the Maturity Method. IOP Conference Series: Materials Science and Engineering, 245(2), 022061. doi:10.1088/1757-899X/245/2/022061.

[90] Yudhistira, A. T., Satyarno, I., Nugroho, A. S., & Handayani, T. N. (2024). Effect of Construction Delays and the Preventive Role of Concrete Works Optimization: Systematic Literature Review. TEM Journal, 13(2), 1203–1217. doi:10.18421/TEM132-34.